

Supporting Information

Lowey et al.

S1 Materials and Methods

Biochemical Procedures. Protein isolation and purification from rabbit tissue, the *in vitro* motility assay, and actin-activated ATPase activity were performed essentially as described previously for mouse cardiac myosin (1).

Construction of a Transgenic Rabbit with the R403Q mutation in the β -Myosin Heavy Chain. RNA was isolated from the apex of a New Zealand White Rabbit heart using RNazol (Molecular Research Center, Cincinnati, OH). Both random primed and oligo dT primed first strand synthesis was performed using SuperScript 2 Reverse Transcriptase (Invitrogen). Primers unique to the rabbit β myosin heavy chain cDNA were used to synthesize the coding region using Herculase II Polymerase (Agilent Technologies). A unique Aat2 restriction site near the middle of the coding region allowed the construct to be assembled in two steps. The R403Q mutation (CGG to CAG) was introduced into the 5' half using overlapping primers that contained the base change. After mutagenesis, the two halves of the construct were assembled using the unique Aat2 restriction site. A 6-His tag was introduced at the beginning of the coding region, immediately behind the start codon. EcoR1 restriction sites were added to the ends of the construct and used to clone the fragment into the rabbit β myosin heavy chain promoter. Isolation of the rabbit β -MyHC promoter has been described previously (2) and a human growth hormone polyadenylation signal was placed downstream (3), digested free of vector sequence with NotI, purified, and used to generate TG rabbits. Fertilized oocyte injections were performed on New Zealand White rabbits as described (4), and the TG rabbits identified using polymerase chain reactions.

The TG rabbits appeared generally healthy and bred normally. Blinded visible and veterinary observations on the rabbits were not able to distinguish the R403Q rabbits from the NTG animals, and sporadic testing using noninvasive modalities such as blood pressure and echocardiography did not reveal any differences. The overall structure of the heart upon sacrifice also showed no notable alterations in structure between the TG and NTG rabbits. Rabbits were housed in an AAALAC approved facility. All experiments were conducted in accordance with the Guide for the Care and Use of Laboratory Animals and approved by the Institutional Animal Care and Use Committee.

Degree of R403 Replacement in the Myosin Heavy Chain. The level of R403Q expression in the TG rabbits was determined by DNA sequencing of the RNA region containing R403 (CGG) in NTG rabbits compared to mutant Q403 (CAG) in the TG rabbits. Expression levels > 40 % of β - myosin are usually lethal, and mice homozygous for R403Q die within a week. We found the transgenic RNA to be 33.7% of the total β -MHC RNA. RNA samples were from 14 week TG and NTG rabbits; the significance of the RNA data was determined by student t-test. It is generally observed that RNA levels do not translate into protein levels; therefore, a value between 10% (from protein isolation, see **Fig. 2**) and 34% (from RNA expression) is a realistic range.

Myofibril Preparations. Small sections of the heart ventricle and soleus were dissected from NTG and TG age-matched rabbits and stored in glycerol/rigor solution (50 mM Tris pH 7.0, 100 mM NaCl, 2 mM KCl, 2 mM MgCl₂, and 10 mM EGTA) containing a cocktail of protease inhibitors (Roche Diagnostics, USA) at -20°C for at least 14 days. The protocol was approved by the Animal Care Committee at McGill University and in accordance with the guidelines of the Canadian Council on Animal Care. On the day of experiments, myofibrils were isolated following procedures developed in our laboratory (5-7). Briefly, a muscle sample was thawed in rigor solution at 4°C for ~1 hour. A small piece was cut out and homogenized twice for 5 seconds at 12,000 rpm and twice for 3 seconds at 28,000 rpm (homogenizer VWR Power AHS250 with a 5 mm generator). This procedure resulted in a solution containing individual myofibrils

and/or small bundles of myofibrils. With the long incubation times at low calcium concentrations, both NTG and TG myofibrils are expected to contain primarily unphosphorylated myosin.

The myofibrils were transferred into an experimental bath containing relaxing solution (pCa²⁺ 9.0) and maintained at 15°C. A myofibril was chosen for mechanical measurements based on its striation appearance, and attached between an atomic force cantilever (AFC; ATEC Nanosensors; stiffness 40.27 nN/μm), and a rigid glass micro-needle connected to a piezo motor, which allowed computer-controlled length changes to the myofibrils. With this system, a laser is shined upon and reflects from the AFC, which deflects when an attached myofibril is shortened due to activation (7). The cantilever deflection is detected and recorded using a newly developed optical system that allows for high time-resolution measurements (8), containing an optical periscope and a photo-quadrant detector with a signal/noise that is reportedly higher than any other system used for experimentation with myofibrils in the literature. Such a system allows precise measurements of force changes during contractions and mechanical manipulation.

Through the experimental procedures, the myofibrils were imaged with an oil immersion 60x magnification microscope objective. The myofibril length, number of sarcomeres, and cross-sectional area were measured at the beginning of the experiments. The myofibrils show a light intensity pattern that represents the contrast between the dark bands of myosin (A-bands), and the light bands of actin (I-bands), allowing for precise measurements of sarcomere length (SL) during experiments. The cardiac myofibrils were set to an average SL of 2.2 μm, and the skeletal myofibrils were set to an average SL of 2.6 μm before activation.

Myofibril activation and mechanical measurements. Myofibrils were activated in pCa²⁺ 4.5 with a multi-channel micro-perfusion system attach to a double-barreled pipette (7-9). When surrounded by a solution containing high Ca²⁺ concentration, the myofibrils produced force, causing deflection of the AFC. The deflection of the cantilever was recorded using an optical system developed in our laboratory (8). The force (F) was extracted from the cantilever displacement and calculated as $F = k \cdot \Delta d$, where k is the cantilever stiffness and d is the cantilever displacement. Forces were normalized by the myofibril cross sectional area, assuming circular geometry.

After the myofibrils were fully activated during the contractions, they were imposed a quick shortening/stretch protocol (amplitude 30%SL; speed 360μm/sec) during which the force declined and rapidly redeveloped to a new steady-state level (7). We analyzed the rate of force development (k_{act}), rate of force redevelopment (k_{tr}) after the shortening-stretch procedure, and the fast phase of relaxation (k_{rel}) during the contractions, parameters that are directly associated with the kinetics of myosin molecules shifting from a weakly bound to a strongly bound (force producing) states (10). For each contraction, k_{act} , k_{tr} and k_{rel} were analyzed with an exponential equation ($a \cdot \exp(-k \cdot (t-c)) + b$), where t is time, k is the rate constant for force development, a is the amplitude of the exponential, and b and c are constants.

Some myofibrils were also tested for the maximal velocity of shortening, and for constructing a force-velocity relation for analysis of power output. First, the myofibrils underwent a slack test: they were allowed to reach maximal force, and a predetermined length step was imposed rapidly (2ms) allowing the myofibril to become slack and tension drop to zero. Force redeveloped over time proportionally to the length change. Four separate slack tests were performed on each myofibril corresponding to length steps of 15%SL, 20%SL, 25%SL and 30%SL. The data was plotted as the time required to re-develop tension relative to the imposed length step, and was fitted with a first-order least squares regression line. The corresponding slope of this fitted line represents the unloaded shortening velocity.

Finally, the myofibrils were released during maximal activation by a step reduction in length (0.007SL/sec - 4 SL/sec). Considering a half-SL (HSL) for ventricles of ~1.1μm and a HSL for soleus of ~1.3μm, length used for the contractions, a velocity of 4.0 SL·s⁻¹ is fast enough to overcome the unloaded cross-bridge cycling velocity (~4.4μm·s⁻¹·HSL⁻¹ and 5.2μm·s⁻¹·HSL⁻¹, for ventricles and soleus, respectively), which causes the force to transiently drop to zero before taking up the shortening. The force at the end of shortening was measured, and Hill's equation was used to fit the force/velocity data for shortening for each myofibril: $(F + a) \times (V + b) = b(F_o + a)$, where a and b are constants, F is force at a

given velocity, V is the velocity, and F_o is the maximal isometric force when $V = 0$. V_{max} occurs when $F = 0$, such that $V_{max} = (b \times F_o)/a$.

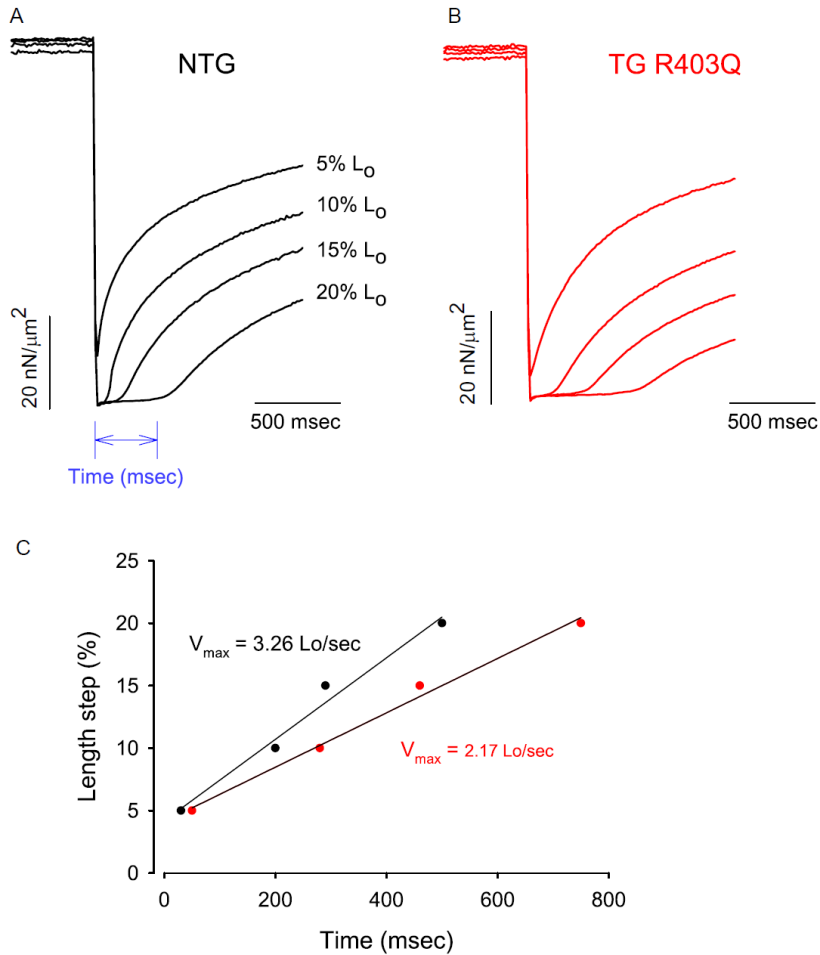


Fig. S1 Traces obtained during experiments investigating the maximum velocity of shortening using the slack test conducted with myofibrils isolated from ventricles from NTG (A) and TG 403 (B) rabbits. The myofibrils were shortened by different magnitudes during full activation; the panels focus on the time during the contraction in which the shortening were applied. The force drops to zero and then redevelops; the time taken for force redevelopment is measured (indicated in panel A). The different times are plotted and the slope of the length step/time relation (panel C) is measured as the maximal velocity of shortening.

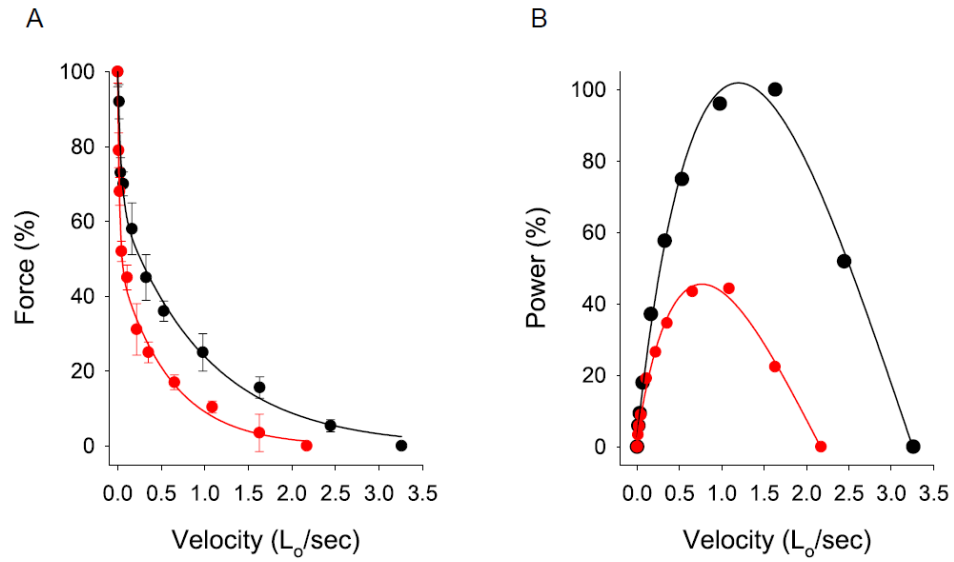


Fig. S2 Force-velocity relation (A) and power-velocity curve (B) before normalization of the velocity to $4.0 L_0$ /sec as shown in Fig. 7 in text. Myofibrils were isolated from NTG (black) and TG 403 (red) ventricles.

Table S1. Actin-activated ATPase activity of rabbit mutant (TG) and non-transgenic (NTG) cardiac myosin subfragment-1.

	V_{\max} (s^{-1})	K_m (μM)
NTG-1	6.6 ± 1.2	47 ± 19
NTG-2	7.6 ± 0.7	30 ± 7
NTG-3	8.4 ± 0.8	51 ± 11
NTG-4	8.9 ± 1.4	47 ± 21
NTG-5	7.7 ± 0.5	47 ± 0.5
TG-6	5.9 ± 0.3	25 ± 4
TG-7	6.0 ± 0.3	26 ± 4
TG-8	5.5 ± 0.3	21 ± 5
TG-9	7.5 ± 0.9	48 ± 1
TG-10	8.5 ± 1.1	67 ± 17

The differences between the V_{\max} of the NTG and TG data sets are not statistically significant ($p=0.065$, t-test).

Table S2. Force and rate constants given in Fig. 6 in text.

	N (rabbits)	N (myofibrils)	Force (nN/μm^2)	k_{act} (/sec)	k_{tr} (/sec)	k_{rel} (/sec)
Soleus NTG	8	62	180.2 \pm 4.82 CI: 170.6 - 189.9	1.76 \pm 0.09 CI: 1.58 - 1.94	1.86 \pm 0.08 CI: 1.69 - 2.04	2.00 \pm 0.10 CI: 1.80 - 2.21
Soleus TG	9	67	138.1 \pm 4.31 CI: 129.5 - 146.7	1.17 \pm 0.06 CI: 1.04 - 1.30	1.22 \pm 0.07 CI: 1.08 - 1.36	1.85 \pm 0.11 CI: 1.63 - 2.07
Ventricle NTG	8	56	117.3 \pm 2.85 CI: 111.6 - 123.0	2.20 \pm 0.07 CI: 2.06 - 2.33	1.99 \pm 0.05 CI: 1.89 - 2.10	4.05 \pm 0.09 CI: 3.87 - 4.23
Ventricle TG	9	71	95.7 \pm 2.54 CI: 90.65 - 100.8	1.40 \pm 0.07 CI: 1.26 - 1.55	1.56 \pm 0.08 CI: 1.41 - 1.72	3.16 \pm 0.16 CI: 2.85 - 3.47

The mean values of force, k_{act} , k_{tr} and k_{rel} for the ventricle and soleus experiments were compared between the NTG and TG myofibrils. CI, confidence interval.

Table S3. Values for the Hill equation before data normalization (see **Fig. S2**).

Parameter	F_0 (nN/μm^2)	V_{max} measured (L₀/sec)	V_{max} predicted (L₀/sec)	a (nN/μm^2)	b (L₀/sec)	a/F_0
NTG	117.3 ± 21.9	3.1 ± 0.9	4.0	30.3	2	0.25
TG	94.6 ± 23.7	1.8 ± 0.4	2.7	34.2	1.4	0.36

After we normalized the curves per maximum force (F_0) and maximum velocity (4.0 L₀/sec) to more clearly compare the two groups of myofibrils, the values of the constant a were 25.1 (NTG) and 38.9 (TG403), the values of the constant b were 1.9 (NTG) and 1.18 (TG403), and the values for a/F_0 , which reflect the curvatures of the curves, were 0.25 (NTG) and 0.32 (TG403).

References

1. Lowey S, *et al.* (2008) Functional effects of the hypertrophic cardiomyopathy R403Q mutation are different in an alpha- or beta-myosin heavy chain backbone. *J Biol Chem* 283(29):20579-20589.
2. Sanbe A, *et al.* (2005) Transgenic rabbit model for human troponin I-based hypertrophic cardiomyopathy. *Circulation* 111(18):2330-2338.
3. James J, *et al.* (2005) Forced expression of alpha-myosin heavy chain in the rabbit ventricle results in cardioprotection under cardiomyopathic conditions. *Circulation* 111(18):2339-2346.
4. James J, *et al.* (2000) Genetic manipulation of the rabbit heart via transgenesis. *Circulation* 101(14):1715-1721.
5. Leite FS, *et al.* (2016) Reduced passive force in skeletal muscles lacking protein arginylation. *Am J Physiol Cell Physiol* 310(2):C127-135.
6. Pun C, Syed A, & Rassier DE (2010) History-dependent properties of skeletal muscle myofibrils contracting along the ascending limb of the force-length relationship. *Proc Biol Sci* 277(1680):475-484.
7. Ribeiro PA, *et al.* (2013) Contractility of myofibrils from the heart and diaphragm muscles measured with atomic force cantilevers: effects of heart-specific deletion of arginyl-tRNA-protein transferase. *Int J Cardiol* 168(4):3564-3571.
8. Labuda A, Brastaviceanu T, Pavlov I, Paul W, & Rassier DE (2011) Optical detection system for probing cantilever deflections parallel to a sample surface. *Rev Sci Instrum* 82(1):013701.
9. Rassier DE (2008) Pre-power stroke cross bridges contribute to force during stretch of skeletal muscle myofibrils. *Proc Biol Sci* 275(1651):2577-2586.
10. Brenner B, Chalovich JM, Greene LE, Eisenberg E, & Schoenberg M (1986) Stiffness of skinned rabbit psoas fibers in MgATP and MgPPi solution. *Biophys J* 50(4):685-691.